polymer reviews

Roles of 'solute' and heat flow in the development of polymer microstructure

J. M. Schultz*
National Chemical Laboratory, Pune 411 008, India
(Received 2 May 1990; revised 12 September 1990; accepted 13 September 1990)

During the crystallization of polymers, both uncrystallizable material (solute') and the heat of fusion are released at the growing interface. Both must diffuse away rapidly enough to permit interface propagation at a velocity (the 'natural' velocity) determined by the thermodynamic driving force. In general, the final microstructure of the solid is determined by the degree to which the flux of solute and heat are compatible with the natural velocity. When the diffusion length $\delta = D/V$ (D = diffusivity, V = interface velocity) is equivalent to or smaller than a dimension of the growing body, diffusional processes control the transformation and the ultimate microstructure. Except for cases of high orientation and relatively large effective undercooling, only solute flow is important. Diffusion solutions for solute flow predict a critical radius, beyond which fibrillated spherulites with solute incorporated between the fibril arms must form. Using a eutectic model, the inter-arm spacing is predicted, with crystallization temperature and diffusivity as governing parameters. Under extreme strain, it is possible for a non-diffusive transformation to take place. In this case, all solute is captured within the growing crystal and the microstructure is governed by the dissipation of the heat of fusion. Very fine, defective fibrillar crystals are predicted. In fibre spinlines, fibrillar crystals grow into a stationary thermal gradient. Modelling of the situation is based on the growth of a thermal dendrite. At each spinline temperature, there is a critical spinline velocity above which crystal growth, in thermal dendrite form, is not possible. This critical velocity dictates the dendrite tip radius. Under these conditions, the fibril diameter must be in the range of 10–100 nm.

(Keywords: microstructure; solute; heat flow)

VARIETIES OF MICROSTRUCTURES IN SEMICRYSTALLINE POLYMERS

There is a large variety of microstructures available to any given crystallizable polymer. Several microstructural types are shown in *Figure 1*. All these structures have been formed by crystallization from the melt. In *Figure 1a* a polypropylene/poly(vinylidene fluoride) (PP/PVDF) blend is shown. Here the PVDF crystallized first as round, smooth-surfaced spherulites; the PP crystallized later, as coarser, concentric spherulites. Of interest here is that spherulites can grow with either a smooth or a serrated front. *Figure 1b* shows greater detail of a PP spherulite growing into a PP melt containing unincorporable chain components. Here it is clear that the front is composed of an array of radial 'arms'. *Figure 1c* shows poly(ether ether ketone) (PEEK) spherulites growing from the surface of a carbon fibre. A dense branching morphology is seen—one in which the spherulitic arms branch profusely to finally form a dense structure. This contrasts with the more regularly armed structures seen in *Figures 1a* and *b*. *Figure 2* shows the microstructure of PP crystallized from a highly oriented melt. One sees here very fine fibrillar crystals oriented in the draw direction. Similar microstructures are seen in melt-spun fibres[1,2].

Within a spherulite there are many levels of microstructure; the two largest are sketched in *Figure 3*. The smaller features in *Figure 3* are ribbon-like or lamelli-form crystals separated from each other by non-crystalline layers. Such interleaved stacks of crystalline and non-crystalline matter have a characteristic spacing of some 10 nm. Such lamellar crystallites appear to be a fundamental growth form, always present within spherulites and with thicknesses reflecting the polymer type and the temperature and pressure of crystallization. At this level, only the interlamellar region is highly affected by non-crystallizable components, these regions acting as 'sinks' for at least a portion of the non-crystallizable material, as indicated by an increase in the thickness of the interlamellar region as the concentration of non-crystallizable species increases[3,4]. The bundles of crystallites, or growth arms, on the other hand, are only sometimes seen. Their presence and lateral dimensions depend on the nature and concentration of any non-crystallizable matter which had been present in the melt and on the solidification temperature. In general, the arm spacing becomes finer with decreasing temperature[5].

It is acknowledged that arm thickness and spacing is defined by the redistribution of non-crystallizable material during crystallization[5–11]. Associated with this is the final location of domains of non-crystallizable material[6,12]. One of the purposes of this paper is to put forward a framework by which spherulitic pattern detail can be treated.

During crystallization, the heat of fusion must be deposited at the growth front. Under conditions of quiescent crystallization, the thermal diffusivity is high enough that dissipation of this heat into the melt poses no hindrance to motion of the growth front. However, if the velocity of crystal growth is sufficiently high, thermal diffusion can also play a major role in pattern

* On leave from the Department of Chemical Engineering and Materials Science Program, University of Delaware, Newark, DE 19716, USA

0032-3861/91/183268-16

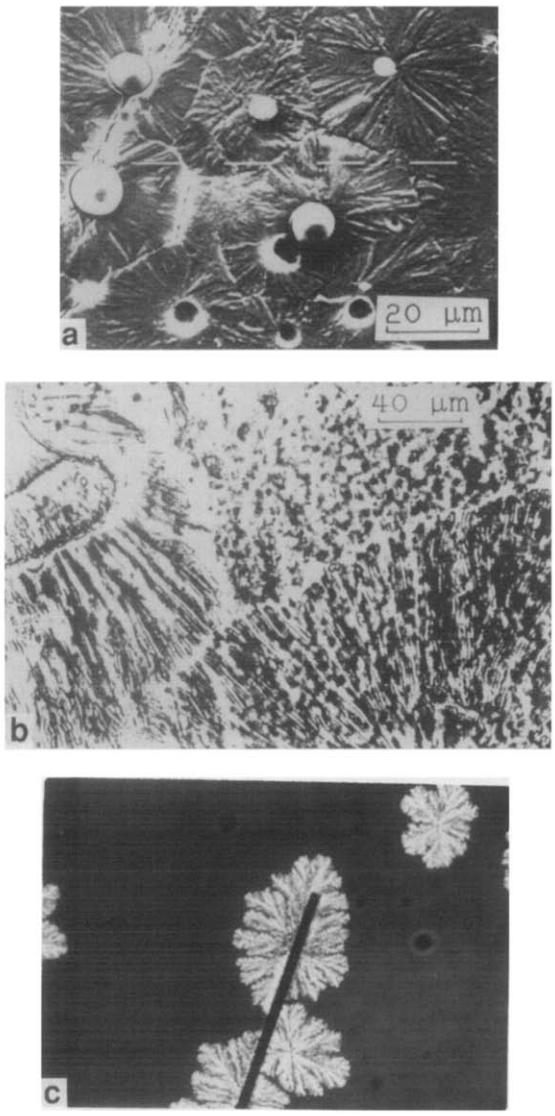

Figure 1 Micrographs illustrating spherulitic microstructures. (a) PP/PVDF blend (50/50), in which the PVDF crystallized first, as spherulites with a smooth spherical surface; PP later crystallized epitaxially on the PVDF spherulites (SEM micrograph). (b) PP spherulite growing into a PP melt (optical micrograph, crossed polarizers). (c) Densely branched PEEK spherulites nucleated on carbon fibres (optical micrograph, bright field)

formation[13]. Such conditions of extreme driving force are expected in the crystallization of highly oriented material. This type of transformation is expected in high-speed spinning, in post-spinning heat treatments of partially oriented yarns and under some laboratory conditions of film formation.

In such cases of rapid, oriented crystallization, transmission electron microscopy of fibres[1,2] and films[14–19] has revealed very fine fibrillar crystals, the fibril axis coinciding with the draw direction. For such cases, solute cannot move rapidly enough to diffuse away from the growth surface and the fine structure is determined by heat flow. Problems of heat flow under such conditions will be discussed.

DRIVING FORCE AND TRANSPORT CONSIDERATIONS

During the crystallization of all materials, two processes must take place: a crystal/non-crystal growth front must move forward, liberating at the interface the heat of fusion and any non-crystallizing species; and the heat of fusion and the non-crystallizing material ('solute') must be conducted away from the growth front.

The crystal/non-crystal front is driven forward by a thermodynamic driving force. This driving force is zero at the thermodynamic melting point, T_m, and increases as the temperature of the non-crystalline phase is depressed further below T_m, i.e. as the undercooling increases. When the driving force for crystallization is low, e.g. at low undercooling, the growth front is driven forward at a low velocity. As the undercooling increases, so does the driving force and the natural velocity, V_n, of the growth front. The growth velocity is an algebraic function of the undercooling $T_m - T$ or ΔT:

$$V_n = V_n(\Delta T) \quad (1)$$

As the growth front moves forward, the latent heat of fusion, L, is evolved continuously at that interface. At the moving front, an amount of heat, LV, per unit area per second is evolved. This heat must be removed, normally by diffusive or convective flow. We note that as the front moves faster and faster, more and more heat is evolved per unit time, requiring increasingly more efficient removal mechanisms.

That dissipative 'solute' flow must be important has also been recognized for nearly 30 years[5–9]. All commercial semicrystalline polymeric materials contain chains which are unincorporable, due to chemical, steric or molecular mass differences. Consequently, concentration effects may be more general in polymers than in low molecular weight materials. If the concentration of some solute in the original non-crystalline phase is c_0 and the (smaller) concentration allowed in the solid is c_s, then

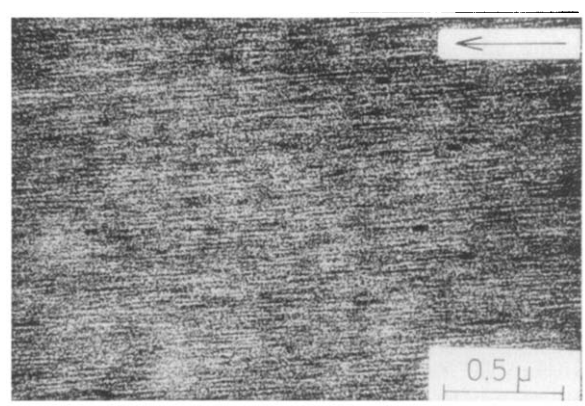

Figure 2 Transmission electron micrograph of a melt-drawn PP film. Draw axis horizontal

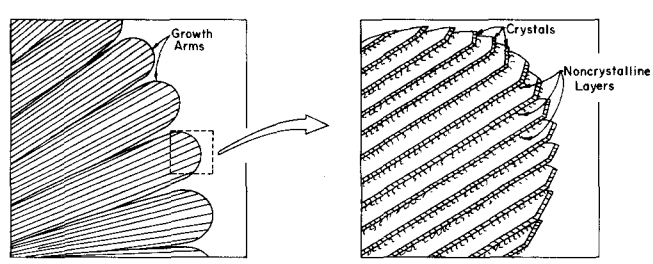

Figure 3 Levels of microstructure in spherulites: (a) spherulite arms; (b) stacked alternating crystalline and amorphous lamellae

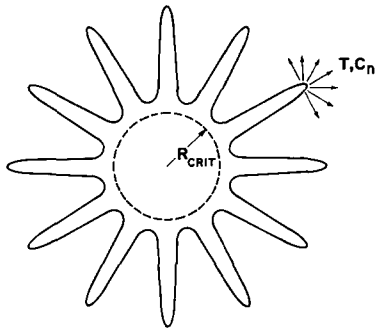

Figure 4 Sketch of the role of sharply pointed asperities in creating three-dimensional diffusion fields

an amount of solute $(c_0 - c_s)V$ is rejected per unit area per second at the interface and must be removed by diffusive or convective action*. Keith and Padden have recently provided a treatment of the effects of chain length effects on the concentration gradient in the melt near the growing interface[8]. The same authors have produced a simplified model for the effect of growth surface geometry on spherulite growth[9]. This latter analysis points to the proper physics but is not sufficiently detailed to provide a framework for a quantitative theory of pattern formation in polymeric systems.

These transport problems provide a limit to the velocity at which the growth front can move forward. Suppose that the transport processes by which the heat or 'solute' is removed are diffusive. A classical problem in diffusivity is that in which a front moves at a velocity V_d, consistent with maintaining thermal and chemical equilibrium at the interface, i.e. with maintaining a temperature T_m at the interface and/or maintaining a thermodynamically specified solute difference Δc across the interface. This diffusion-limited velocity V_d is that which would be taken by the system when the role of the driving force is ignored, i.e. when V_n is so much greater than V_d that growth dynamics are determined only by V_d.

At low driving forces, V_n is low. If $V_n \ll V_d$, then heat and 'solute' can diffuse away easily and V_n becomes the velocity of the interface. At very high driving forces, $V_n > V_d$ and transport of heat and/or solute control the behaviour. Under these circumstances, the system seeks means whereby heat and solute can be removed most efficiently. Increasing this efficiency usually means changing the removal process from one-dimension (as for a planar front or, nearly, for a spherical one) to a greater dimensionality. *Figure 4* illustrates the nearly 4π solid angle available to solute or heat flow in protuberant growth.

When $V_n > V_d$, the interface becomes unstable to protuberances and the ultimate growth takes place via rod-like or lamellar growth entities. Fascinating and interesting growth patterns such as dendrites, spherulites and two-phase growth forms occur. The underlying physics for these processes has been studied for many years. The generic name for such processes is 'pattern formation' during crystallization[20].

It is the aim of this study to treat pattern formation in polymer crystallization. For the most part, the models will be kept as simple as possible, so that the conceptual physics and their quantitative application are clear. We shall consider the underlying physics, and then the role of the material and thermal fields in pattern formation in the quiescent crystallization of homopolymers and blends and for the case of strain-assisted crystallization, especially fibre spinning.

DRIVING FORCE AND THE NATURAL GROWTH VELOCITY

At any temperature below the equilibrium melting point, a melt is unstable with respect to the crystalline phase. The free energy decrement upon crystallization of a (boundless) mass of material is given approximately by:

$$\Delta G_{c/n} = L(T_m - T)/T_m \qquad (2)$$

where $\Delta G_{c/n}$ is the free energy difference between the crystalline and non-crystalline phases and T is the temperature at which the transformation is taking place. The quantity $T_m - T$ is termed the 'undercooling'.

Kinetic rather than purely thermodynamic factors govern the rate of this transformation, and indeed whether or not the transformation will take place within a measurable time at a given temperature or at a given cooling rate. The kinetics of the forward motion of the crystal/non-crystal interface relate to the rate at which new matter is deposited on the growing face of the crystal. *Figure 5* shows the growth surfaces of lamellar crystals. Growth occurs by the accretion of chain strands onto the growth surface. Suppose that the growth surface is initially smooth, i.e. a layer of chain strands has just been deposited and a new one has not yet been started. The new layer starts, as in *Figure 5a*, with the deposition of the first strand. This first strand is bound to relatively few neighbours in the already completed layer. Thus it lowers the internal energy of the system only a little, compared to a strand wholly incorporated within the crystal. On the other hand, this strand (and every strand) adds an amount of surface energy $\gamma_e v_s$, where γ_e is the specific surface energy of the broad surface and v_s is the cross-sectional area per strand. The result is that there is a net increase in internal energy upon depositing the first strand. Subsequent strands bind to already placed strands in the new layer, as well as to the substrate layer and consequently lower the net internal energy. For both the first and the subsequent strands, the chain segments must be transported from the non-crystal side of the interface to the crystal side and there is also an activation energy of transport, Q_t, to be overcome.

Thus for both the deposition of the first strand and of the ensuing strands there is an activation energy to be overcome by thermal fluctuation. The activation energy for the initial strand is much larger than that for the strands which will complete the layer. One can describe this total process in terms of sequential nucleation (deposition of the first strand) and layer growth (deposition of the following strands). Hoffman *et al.*[21] have observed two distinct kinetic regimes in the crystallization of polymers from the quiescent melt. At

* Intrachain defects, including chain ends, are normally unincorporable or are incorporable only at low concentrations in polymer crystals. The conduction of defects away from the growing interface can be important at the dimensional level of the interdefect spacing. This would be some 10 nm for cases of interest and consequently the crystalline thickness, of the same order of magnitude, could be affected. In the present context, however, only larger dimensional levels are considered and questions of defect flow will not be treated

relatively low supercoolings, the rate of nucleation is relatively small, compared to the layer growth rate. In this case, once a new layer nucleates, layer growth to complete the layer occurs very rapidly and then a new layer must once again be nucleated. This regime I process is illustrated in *Figure 5a*. At lower temperatures, regime II, the absolute rates of nucleation and layer growth become competitive and new layers nucleate on growing layers. This situation is depicted in *Figure 5b*. The overall growth velocity, V_n, is analysed according to a kinetic analysis due to Lauritzen and Hoffman[22,23], based on an earlier model of Turnbull and Fisher[24]. This analysis results in the following expression, which is valid in both regimes I and II[21]:

$$V_n = A \exp[-Q_t/R(T - T_1)] \exp(-K_g/T\Delta T) \quad (3)$$

where A is a constant, T_1 is a temperature somewhat below the glass transition temperature and K_g is the net activation energy for layer growth (a compound of the nucleation and layer growth activation processes). Clearly, the first exponential represents transport across the interface and the second exponential represents deposition of strands on the crystal. Here K_g has different expressions in regimes I and II:

$$\text{Regime I:} \quad K_{gI} = 4B\gamma_e\gamma_s T_m/kL \quad (4)$$

$$\text{Regime II:} \quad K_{gII} = 2b\gamma_e\gamma_s T_m/kL \quad (5)$$

where b is the thickness of a layer and k is Boltzmann's constant.

Two comments on equations (3)–(5) are useful at this point. (1) The natural growth velocity is the product of a transport term, $\exp[-Q_t/R(T - T_1)]$, and a driving force term, $\exp(-K_g/T\Delta T)$. The transport term increases monotonically with temperature, whereas the driving force term increases with undercooling (at least until rather high levels of ΔT). The product of these two terms produces the familiar bell-shaped dependence of growth velocity on temperature. (2) There is no reliable way to determine the constant A from elementary material constants or fundamental properties. Consequently, throughout our study, when absolute values of V_n are required, we shall resort to empirical results.

The empirical data for homopolymers comes from spherulite growth rates measured at small undercoolings. *Figure 6* gives spherulite growth rate curves for polymers to be discussed further in this work. We will take growth velocities measured at temperatures between the growth rate maximum and the melting point to approximate V_n.

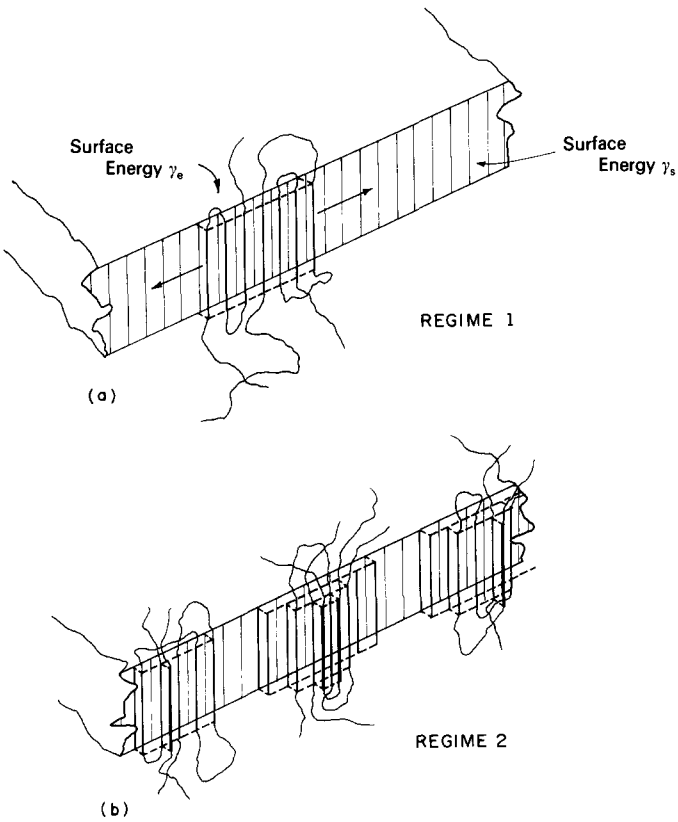

Figure 5 Models of crystal growth due to the accretion of chain strands onto the lateral surface of a thin polymer crystal: (a) regime I, in which a new layer is completed before the next layer begins; (b) regime II, in which there is simultaneous growth from several centres and layers

DIFFUSION LIMITATION OF THE VELOCITY OF A BROAD INTERFACE

Solutions to the diffusion equation

The question is 'At what velocity can an interface move forward when it liberates heat or solute which must be transported away?' This is a classical diffusion problem and will be summarized here.

For reasons of simplicity, we will treat first a pure solid growing into a pure melt supercooled to temperature T_0. We will then modify this result for the case of solute diffusion. For the moment, we will treat the case in which

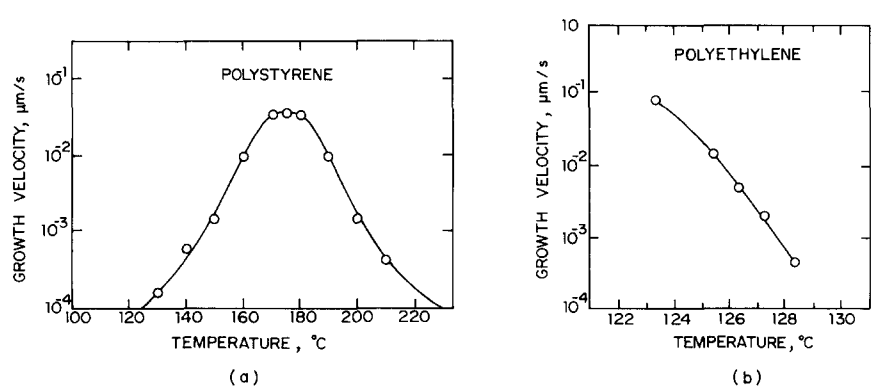

Figure 6 Measured spherulite growth rate *versus* temperature for polymers discussed in the present work: (a) 90:10 iPS/aPS blend[28]; (b) 80:20 high/low molecular weight blend of high density polyethylene[35]

the solid remains infinitesimally below T_m and all heat is transported into the melt. Consider a planar crystal/non-crystal interface moving forward at velocity V into a melt at temperature $T < T_m$. The amount of heat liberated per unit time per unit area of interface is LV. This flux of heat must be proportional to the thermal gradient $(dT/dx)_0$ at the surface, given an origin of coordinates in the interface:

$$VL = -D_T(dT/dx)_0 \quad (6)$$

As the interface moves forward, the temperature at each distance x ahead of the interface is given by Fourier's law:

$$dT/dt = -D_T(d^2T/dx^2) \quad (7)$$

The solution to equation (7) which is consistent with equation (6) and with the boundary condition

$$T \to T_0 \quad \text{as} \quad x \to \infty \quad (8)$$

is[25]:

$$V = \lambda(D_T/t)^{1/2} \quad (9)$$

where λ is given by

$$\lambda^2 \exp(\lambda^2)\operatorname{erfc}(\lambda) = (T_m - T_0)c_p/\pi^{1/2}L \quad (10)$$

where c_p is the specific heat of the non-crystalline phase. Here $\operatorname{erfc}(\lambda) = 1 - \operatorname{erf}(\lambda)$, where $\operatorname{erf}(\lambda)$ is the tabulated error function[26].

For solute rejection, the analysis is exactly as above. The amount of solute rejected per unit area per second is given by $V[c_n(\text{int}) - c_s]$, where c_s is the (constant) solute concentration in the solid and $c_n(\text{int})$ is the solute concentration in the non-crystalline phase at the interface, in equilibrium with c_s. The flux equation at the interface becomes

$$V[c_n(\text{int}) - c_s] = -D_s(dc_n/dx) \quad (11)$$

The far-field boundary condition is

$$c_n \to c_0 \quad \text{as} \quad x \to \infty \quad (12)$$

Fick's second law is

$$dc_n/dt = -D_s(d^2c_n/dx^2) \quad (13)$$

And the solution is

$$V = \lambda(D_s/t)^{1/2} \quad (14)$$

where

$$\lambda^2 \exp(\lambda^2)\operatorname{erfc}(\lambda) = \{[c_n(\text{int}) - c_0]/[c_n(\text{int}) - c_s]\}/\pi^{1/2} \quad (15)$$

A similar treatment applies to a spherical growth front. The solutions in this case for heat and solute rejection, respectively, are again given by equations (9) and (14) but now with

$$\lambda^2 - \pi^{1/2}\lambda^3 \exp(\lambda^2)\operatorname{erfc}(\lambda) = c_p(T_m - T_0)/2L \quad (16)$$

$$\lambda^2 - \pi^{1/2}\lambda^3 \exp(\lambda^2)\operatorname{erfc}(\lambda) = \{[c_n(\text{int}) - c_0]/[c_n(\text{int}) - c_s]\} \quad (17)$$

Evaluation of diffusion-limited velocities will be treated presently.

Diffusion length

The diffusion length is the distance over which a concentration or temperature field decays to 1/e of its value at some origin. In the present case, we consider heat or solute being input at the planar surface of a semi-infinite solid. The constant rate of input is $V_dL\rho_m$ or $V_d(c_0 - c_s)$, where ρ_m is the density of the non-crystalline phase. Suppose this input to be constant in time and the interface be stationary. The problem is then given by:

$$\begin{aligned} LV_d/c_p &= -D_T(dT/dx)_{x=0} \\ V_d(dT/dx) &= -D_T(d^2T/dx^2) \end{aligned} \quad (18)$$

or

$$\begin{aligned} (c_0 - c_s)V_d &= -D_s(dc_n/dx)_{x=0} \\ V_d(dc_n/dx) &= -D_s(d^2c_n/dx^2) \end{aligned} \quad (19)$$

The solutions to equations (18) and (19) are, respectively:

$$[T(x) - T_0]/[T(0) - T_0] = \exp(-V_dx/D_T) \quad (20)$$

and

$$[c_n(x) - c_0]/(c_0 - c_s) = \exp(-V_dx/D_s) \quad (21)$$

In both cases, the left-hand side is the fractional decrease in level between the value in the melt at the interface and the far-field value. When the left-hand side of equation (20) or (21) is 1/e, the value of the diffusion length δ is defined by:

$$\delta = D/V_d \quad (22)$$

where D is either D_T or D_s.

A very long diffusion length indicates that diffusion will have little effect on pattern development. A small value of δ indicates that solute or heat diffuses with difficulty and may be a significant effect in solidification. 'Large' or 'small' here refer to some characteristic dimension of the growing object.

For molten polymers, D_T is usually near 1×10^{-3} $cm^2\,s^{-1}$ and D_s is normally in the range 10^{-14}–10^{-10} $cm^2\,s^{-1}$. A typical spherulite growth velocity is of the order 10^{-6} $cm\,s^{-1}$. Thus the thermal and solute diffusion lengths are approximately:

$$\delta_T = 10^3\ \text{cm} \qquad 10^{-8} < \delta_s < 10^{-4}\ \text{cm}$$

Thus thermal diffusion has no bearing on spherulitic crystallization, whereas solute diffusion should be a factor involved in pattern formation during quiescent crystallization.

Thermal diffusion can be important, however, when the driving force is very high and growth velocities are of the order of 1 $cm\,s^{-1}$ or higher. Very high growth velocities are experienced in fibre threadlines and post-spinning heat treatments. In such cases, the thermal diffusion length is of the order of microns or smaller and the solute diffusion length is of sub-Ångstrom dimensions. Clearly, no transformation should take place under these conditions unless the solute is accepted within the crystal. Under such high driving forces it is possible that very defect-laden crystals would form, if that were necessary to allow a growth front to move forward. In such cases of rapid, oriented crystallization, transmission electron microscopy of fibres[1,2] and films[14–19] has revealed very fine fibrillar crystals, the fibril axis coinciding with the draw direction and the as-grown crystals being very defective[18,19,27]. For such cases, the fine structure is determined by heat flow.

In the following, the question of solute redistribution during spherulitic crystallization will be addressed and

we shall look at the case of crystallization under extreme orientation, where solute incorporation should occur and thermal fluxes become controlling for pattern formation.

STABLE AND UNSTABLE SPHERICAL SURFACES

Statement of the critical radius problem

In *Figure 1* we saw the smooth, stable spherical growth surface of PVDF and the unstable, protruberant growth of PP and PEEK. A first question to be answered is 'Under what conditions are stable and unstable spherulite growth to be expected?'

There are two approaches to answer this question. In one approach, one asks whether V_d is sufficiently large to keep pace with V_n. If the answer is 'yes', then the interface is stable; if 'no', then it is unstable. The other approach is to use a formal 'interface stability' approach. The former approach is used here.

Using the best available values of diffusivities, values of λ are computed from equation (17). Actually, upper and lower bounds are found, as will be shown below. From equation (14) and $R = \int_0^t V_d \, dt$, we write:

$$V_d = 2\lambda^2 D_s / R \qquad (23)$$

Using equation (23), we compute V_d as a function of R. The sphere radius for which V_d is approximately equal to V_n is the critical value for transition from a stable (at small R) to an unstable (at larger R) interface.

Evaluation of V_d

Two practical problems are encountered in carrying out this simple analysis.

The most difficult part of such an evaluation is to locate reliable, absolute values of the diffusivities D_s. Recent development of measurement methods has enabled accurate measurement of such diffusivities. These new measurements have generally shown that older data are in error by orders of magnitude. Consequently, one is limited to a relatively few polymers and temperatures for which diffusivities have recently been measured, using Rayleigh backscattering, small-angle neutron scattering or fluorescence tracer methods. Most of these measurements relate to self-diffusivities in homopolymers, although some blend data are also available.

While spherulite growth data for many homopolymers are available, information on blends or polymer-diluent systems is scanty and little diffusivity data is available for these systems.

For the above reasons, the number of systems currently available for computation is small.

A third problem is that a theoretical prediction of $c_n(\text{int})$ is difficult to obtain. Because of this, evaluation of the right-hand side of equation (17) is similarly difficult. It is, however, possible to place upper and lower bounds on the right-hand side of equation (17).

The upper bound is found as follows. Since c_s must be much smaller than either c_0 or $c_n(\text{int})$, the right-hand side of equation (17) is approximately $(1/2)[1 - c_0/c_n(\text{int})]$. The highest conceivable value of $c_n(\text{int})$ is 1. Thus the maximum value of the right-hand side is $(1 - c_0)/2$.

The lower bound is found from consideration of a stationary plane, at whose surface is generated a flux of solute equivalent to that of the moving interface considered above. In this case, $c_n(\text{int}) = 2c_0 - c_s$ [obtained from equation (21)].

One system for which data is available is isotactic/atactic polystyrene (iPS/aPS) blends. Spherulite growth velocities are available for such blends[6,28] and self-diffusivity measurements of iPS[29–31] are among the best available for any polymer. Furthermore, the growth rate and diffusivity measurements have overlapping ranges of molecular weight and temperature. One must assume, however, that the diffusivities of both moieties in the blend have approximately the measured aPS diffusivity.

Another system for which reasonable data are available is that of high-density polyethylene (HDPE) blends. Excellent recent diffusion data, based on infra-red microdensitometry[32,33] and on small-angle neutron scattering[34], are available. Included in these data are some results on HDPE blends[32]. Rego Lopez *et al.*[35] have reported spherulite growth rates for blends of HDPE having weight-average molecular weights of 66000 and 2500.

Let us now look at the case of PS. It should be a good approximation that no atactic molecules can be incorporated into iPS crystals. Suppose then that all the atactic material excluded from the crystal is pushed ahead of the spherulite; that is, none is incorporated into the spherulite. (The case in which some incorporation can occur turns out to be important and will be treated later.) In this case, the requisite concentrations for comparison with measured spherulite growth rates in a 90/10 iPS/aPS blend are: $c_s = 0$, $c_0 = 0.1$ and $0.25 < (1/2)[1 - c_0/c_n(\text{int})] < 0.45$.

Using these values, one computes λ from equation (17). Using this value of λ, one computes V_d *versus* R from equation (23). In this latter step a diffusivity of 2.0×10^{-13} cm^2 s^{-1}, corresponding to a molecular weight of 190000 at 174°C[30] has been used. The computed V_d values can be compared directly with spherulite growth rates measured by Boon *et al.*[28] for a similar system ($M_\eta = 330000$, $c_0 = 0.1$, $T = 175$°C), $V_n = 0.22$ μm s^{-1}).

One can similarly compute λ, and V_d *versus* R for polyethylene blends. At temperatures above 120°C, the low molecular weight species ($M_w = 2500$) is entirely excluded from the growing crystals[35]. Considering an 80:20 ratio of high (66000) to low molecular weight material, one can again approximate the concentration conditions: $c_s = 0$, $c_0 = 0.2$ and $0.25 < (1/2)[1 - c_0/c_n(\text{int})] < 0.40$.

For crystallization[34] at 125°C, $D_s = 1.2 \times 10^{-10}$ cm^2 s^{-1}. This is the self-diffusivity of the higher molecular weight species. Since Klein has shown very little dependence of diffusivity on matrix molecular weight[33], even when the matrix is of much lower molecular weight, this value should be a good approximation for the blend. In the comparisons given below, spherulite growth velocities are taken from Rego Lopez *et al.*[35].

In *Figure 7*, computed values of the minimum and maximum possible growth velocities are plotted against the spherulite radius for a 90/10 iPS/aPS blend. Shown also is the measured growth rate for this system[28]. What are chiefly to be noted are the following: the diffusion-limited growth velocity V_d decreases as the spherulite grows, $V_d \propto 1/R$, contrary to most measurements, which indicate a constant velocity; at submicron spherulite radii V_d becomes much smaller than the actual

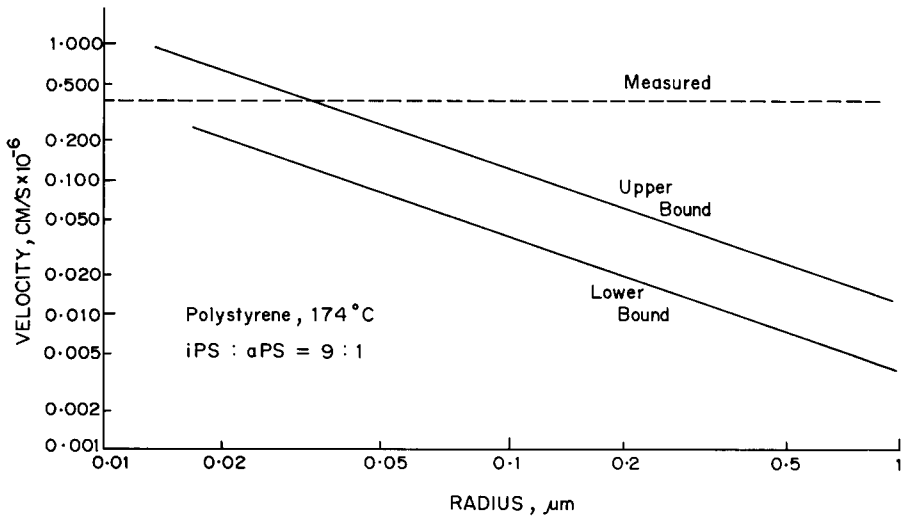

Figure 7 Computed diffusion-limited spherulite crystallization velocity *versus* the instantaneous radius of a spherulite growing at 174°C in 90:10 iPS/aPS blend. Also shown is the measured spherulite velocity

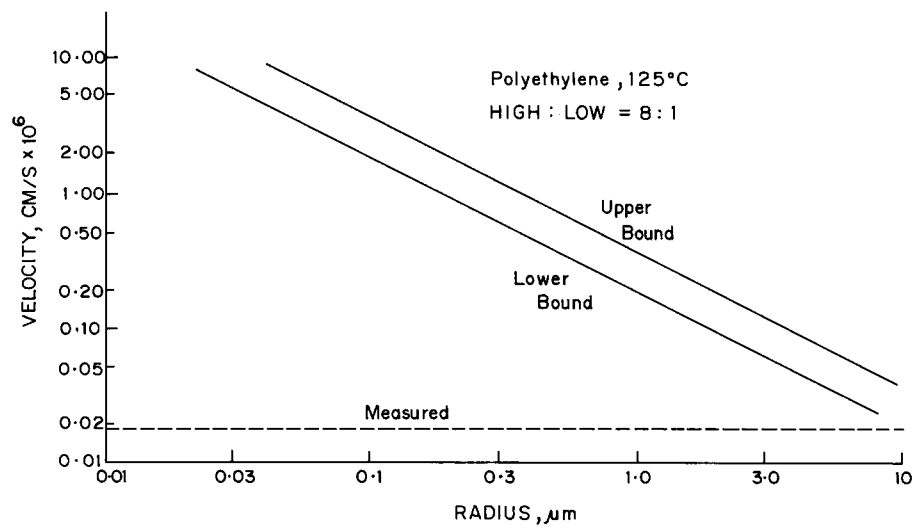

Figure 8 Computed diffusion-limited spherulite crystallization velocity *versus* the instantaneous radius of the spherulite growing at 125°C in 80:20 high/low molecular weight high density polyethylene blend. Also shown is the measured spherulite velocity

velocity. The V_n, associated with the thermodynamic driving force, is very large and has forced the interface to move at a velocity beyond that at which a simple spherical interface is stable. Such a surface becomes unstable to protuberances, which grow at a much faster velocity.

Figure 8 shows the computed minimum and maximum diffusion-limited growth rates of spherulites in a 80/20 blend of high and low molecular weight linear polyethylene. Also shown are the measured spherulitic growth velocities. In this case, spherulites grow to a much larger size before fibrillation sets in. This growth to a larger size is due to the smaller diffusivity of polyethylene as opposed to PS. Here the non-crystallizable molecules diffuse away more rapidly and a higher velocity must be reached before the build-up of solute at the interface is high enough to require the growth of sharp asperities.

The critical radius for spherical stability depends on the growth temperature and on the molecular weight of both components. In *Figure 9* are shown velocity–radius plots for an 80/20 polyethylene blend, for three different temperatures. Over the temperature range considered (123–128°C) V_n changes by several orders of magnitude, whereas V_d is little affected. What is seen is that the critical radius increases with growth temperature. In *Figure 10* are shown the spherulite microstructures one would expect for the three solidification temperatures in *Figure 9*. At the highest temperature, a spherulite of 6 μm diameter would have occluded all solvent, whereas at the lowest temperature the spherulite diameter at which incorporation of solvent must occur is so small that it would not be observable. In this way, the transformation temperature is a critical variable in pattern formation in blends.

The molecular weights of the components are likewise important variables. Equation (23) shows that the velocity at any radius value scales as the diffusivity for diffusion of solute from that surface. Thus the computed curves for diffusion-limited growth in *Figures 7* and *8* will be shifted up or down, depending on the value of D_s. *Figure 11* illustrates this effect for high/low linear polyethylene blends with three different diffusivities, corresponding to three different molecular weights. As the molecular weight is increased (and the diffusivity correspondingly decreased), the V_d values cross the V_n line at decreasing values of spherulite radius. In fact, the

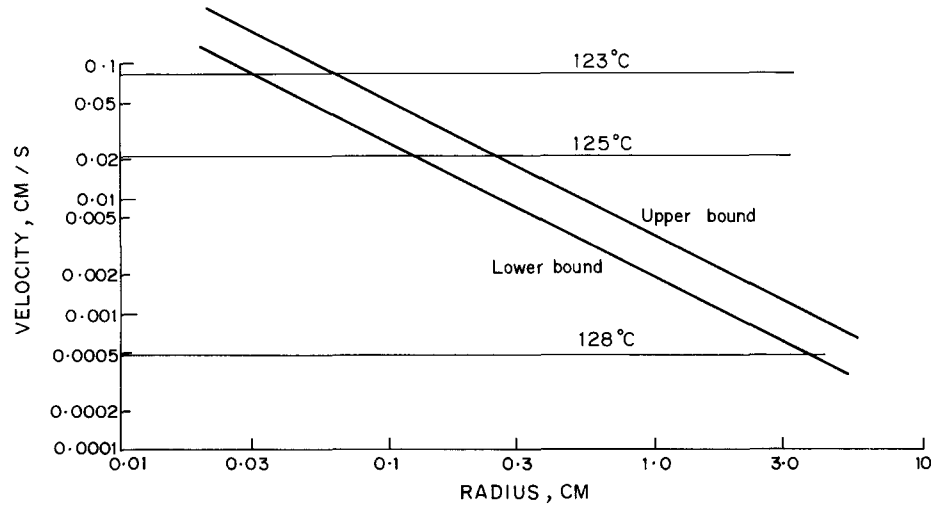

Figure 9 Computed diffusion-limited spherulite crystallization velocity curve for 85:15 high/low molecular weight HDPE but showing now the effect of crystallization temperature on the natural (measured) growth rate and the limiting size of a smooth-surfaced spherulite

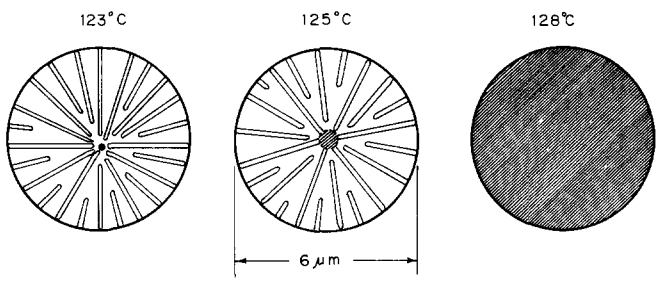

Figure 10 Scale model of the relative sizes of the smooth-surfaced portions of spherulites which have grown to a 6 μm diameter. The critical size is taken from *Figure 9*

V_n line will also shift somewhat with molecular weight but this will be a relatively small effect compared with the shift of the diffusion-limited growth curves.

If the equilibrium melting point of the blend is significantly affected by the solute, then the driving force and V_n at a given temperature will likewise depend upon concentration. Such effects also need to be accounted for.

Comments on interface stability

The stability of a growing planar or spherical interface has been a subject of theoretical treatment and of simulation for nearly 30 years[36–44]. In such work, the interface is subjected to a small modulation of prescribed form and the system interrogated as to whether or not the modulation will develop more rapidly than the smooth interface. Any modulation will provide more efficient solute or heat diffusion. Consequently, any modulation will grow, if not resisted by the creation of surface energy. If one considers the modulations to be linear or spherical surface waves, the surface energy restricts growing modulations to be above a certain wavelength. The fastest growing wavelength can also be identified, as can the maximum size to which a sphere can grow before becoming unstable.

Calvert[10] has applied these considerations to spherulite front stability in polymers. He concludes that for any reasonable value of diffusivity the spherical front is unstable relative to a fibrillar front.

The applicability of such stability analysis to spherulitic growth is somewhat dubious. In a footnote to a recent paper, Keith and Padden[45] point out that the interface between crystalline and non-crystalline regions has *ab initio* existence within a spherulite and that, consequently, new surface is not formed at an unstable growth front. This condition is shown schematically in *Figure 12*. Here, any surfaces which form during surface modulation would form similarly during the motion of a spherical front. The total surface area is given by the spherulite volume and the intraspherulitic lamellar spacing. If there is actually no surface energy contribution there should be no lower limit to the fineness of the surface modulation. The conclusion to be reached from this argument is that the spherical growth front is inherently unstable and that the spacing of outgrowing asperities must be governed by solute and/or thermal fluxes directly. Our attention is therefore directed at how such fluxes may determine the growth patterns formed.

OVERVIEW OF SPHERULITE PATTERN FORMATION

Consider now that a spherulite has nucleated and begun to grow. As it begins, it is nearly a 'point source' of heat or solute. As it grows, its radius of curvature becomes larger, and the spherulite behaves increasingly like a growing plane. If the driving force is sufficiently large, at some radius level solute cannot diffuse away fast enough to maintain the natural growth rate of the spherulite.

At this point, it may be envisioned that any of three things may occur:

1. The growth may slow down. In this event, there is an unfulfilled driving force, waiting to propel the growth front at a faster velocity, if an opportunity is presented.
2. The growth front may decompose into an array of narrow, rod-like or lamellar protuberances, growing monotonically outward and leaving more and more space between themselves. A variant is that these narrow entities, still growing independently of each other, generate equally narrow branches, which act to fill the space between the principal trunks. In such cases, the solute molecules diffuse away very rapidly, but a relatively sparse spherulite is formed, unless some additional space-filling mechanism comes into play.

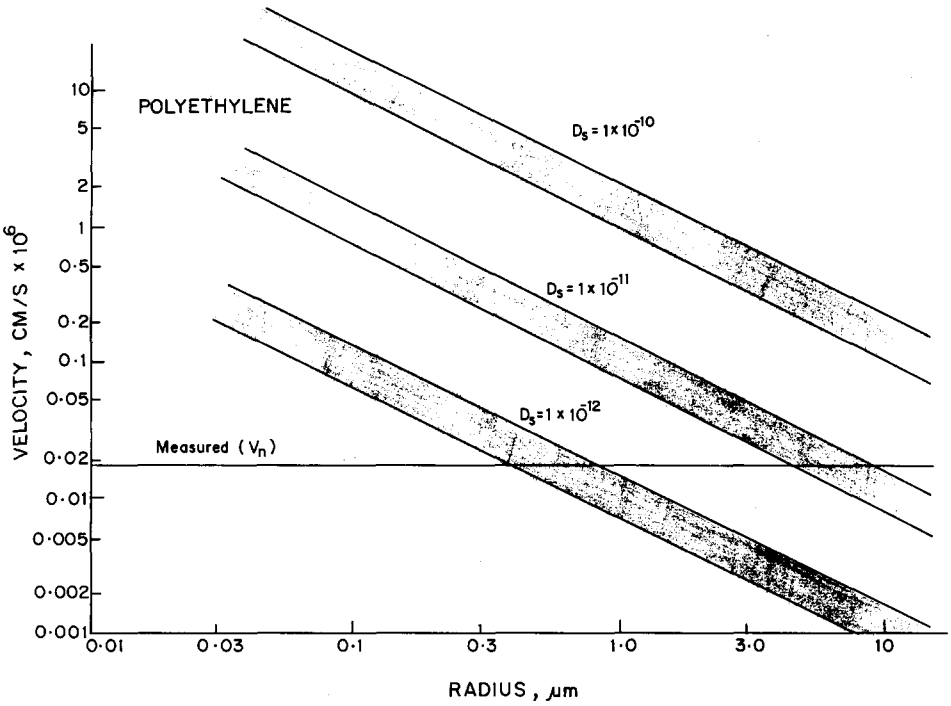

Figure 11 Computed diffusion-limited spherulite crystallization velocity curve for 80:20 high/low molecular weight HDPE but showing now the effect of molecular weight (as manifest in the diffusivity) on the natural (measured) growth rate and the limiting size of a smooth-surfaced spherulite

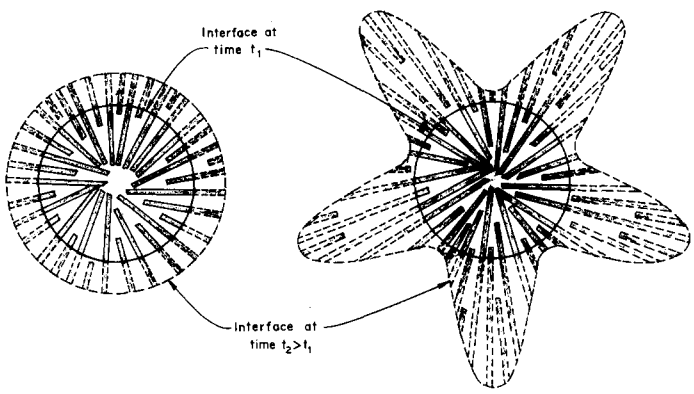

Figure 12 Schematic figures showing a smooth-surfaced spherulite and one with pronounced growth arms. What is to be noted is that in the spherulite with arms there is no new crystal/amorphous surface formed, relative to a similar volume of smooth spherulite, since each crystallite is surrounded by amorphous matter in both cases

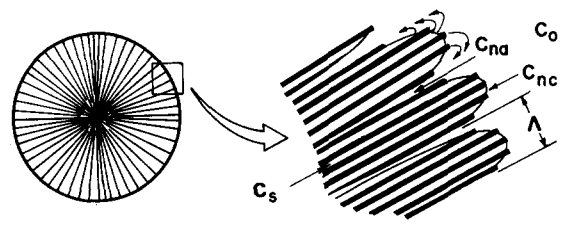

Figure 13 Sketch showing concentrations, diffusion directions (curved arrows) and arm spacing (Λ) in a polymer spherulite

3. The growth front remains macroscopically coherent, but is microscopically broken up into transformed and untransformed regions (Figure 13). In this case, the untransformed regions can act as sinks for the solute excluded from the transformed regions. In this way, solute need not be transported into the far-field, but rather need only be transported over a distance of some $\Lambda/2$, half the periodicity of the untransformed regions.

Consider now what happens as a tiny spherulite grows. As it expands, more and more solute is excluded and the solute concentration $c_n(\text{int})$ near the interface builds up. At the same time, the diffusion geometry becomes increasingly linear, because of the increase in radius (decrease in curvature). At some radius level, the solute flux beyond a spherical interface can no longer keep up with the driving force. So long as some path toward faster solute transfer is available, the interface will not slow down over its entire surface, but rather the spherical interface becomes unstable to perturbations. Since surface energy is probably not a hindrance, there is no lower limit to the wavelength of viable surface modulations. Because the growth of surface modulations increases as the modulation becomes finer and finer, it is expected that nature will choose the finest asperities consistent with the interference of solute fluxes from adjacent asperities. That is, what limits the fineness of the resulting microstructure is the interference of the solute fields of adjacent asperities. Thus, of the three possibilities above, the third is normally preferred. This situation resembles very closely that encountered in eutectic solidification of low molecular weight materials.

It is useful to point out, however, that whether solution (2) or (3) is more likely depends on whether or not the spherulite can break down into closely spaced asperities. Such a fine structure must depend on the concentration of non-crystallizable material. If the overall concentration of non-crystallizable material is c_0, if the concentration in the crystallites is zero and if the concentration of non-crystallizable material in the domains between asperities can be 1, then a mass balance shows the ratio of asperity width to intervening width to be $(1 - c_0)/c_0$. Consequently, for blends which are dilute in the crystallizable component, the growing asperities must be widely separated. In this case, one would expect growth

according to case (2): independent dendrites. Indeed, this situation is found in such dilute blends, as seen in Keith and Padden's dilute iPS/aPS materials[6].

'EUTECTIC' CRYSTALLIZATION OF SPHERULITES

The separation of 'solute' at the growth front may be very similar to what occurs in eutectic alloys of small molecule systems. A material with a eutectic transformation exhibits a phase diagram of the type shown in *Figure 14a*. If an alloy of composition c_0 is cooled from the melt through the eutectic temperature T_{eu}, two new phases must form simultaneously. In general, such transformations occur by the coupled growth of either alternating plates of the two phases or of rod-like crystals of one phase within the other. The growth of alternating lamellae is sketched in *Figure 14b*. The reason for the formation of such a fine, coupled growth is that only by such means can diffusion keep pace with V_n. Since the α phase is immediately adjacent to the β phase at the growth front, A and B components need be transported over a distance of only some $\Lambda/2$, where Λ is the periodicity of the α–β stacking.

A proper quantitative understanding of such a coupled transformation requires treatment of the coupled growth of dendrites with overlapping compositional fields. This topic has been treated extensively elsewhere[46–50]. An exact analytical solution is difficult and there is as yet no agreement on an optimization principle.

A first-order, quantitative solution can be taken from an older, simpler model[51]. In this model, the empirical result that growth is steady state is used. In this situation one can use Fick's first law to model the diffusive process beyond the growing edges. The flux of solute to be transported away is $J = V_{eu}(c_0 - c_B)$, where c_0 is the far-field concentration of B in the melt and c_B is the concentration of B in solid α phase. This flux is proportional to the concentration gradient, which is now approximately $(c_{B\alpha} - c_{B\beta})/\Lambda$, where $c_{B\alpha}$ and $c_{B\beta}$ are the concentrations of B in the melt just at the α/melt and β/melt interfaces, respectively. The form of the solution is then:

$$V_{eu}(c_0 - c_B) = D(c_{B\alpha} - c_{B\beta})/\Lambda \quad (24)$$

Suppose now that crystallization of a polymer blend occurs through the creation of two new phases, platelets of solute-free crystalline lamellae, separated from each other by a non-crystalline ('amorphous') phase of composition c_a, into which all excluded solvent has been incorporated. This system is sketched in *Figure 13*, along with illustrative diffusion paths for the excluded material. The composition of the non-crystalline phase in contact with the crystalline phase is c_{nc}; that in contact with the amorphous, intervening layer c_{na}. Here, V_{eu} is equated with V_n. Following the simplified treatment of equation (24):

$$V_n[c_0 - c_s] = -D_s[c_{nc} - c_{na}]/\Lambda \quad (25)$$

If we now take $c_0 \gg c_s$ and $c_{nc} \gg c_{na}$, then:

$$V_n \cong D_s(c_{nc}/c_0)/\Lambda \quad (26)$$

From equation (21), we see that c_{nc}/c_0 has a lower limit of 2. Thus:

$$(V_n)_{min} = 2D_s/\Lambda \quad (27)$$

The absolute upper limit of c_{nc}/c_0 is $1/c_0$. Thus:

$$2D_s/V_n < \Lambda < D_s/c_0V_n \quad (28)$$

Keith and Padden[5,45] considering cellulation at the growth front, arrive at the same functionality.

While D_s and V_n are strong functions of temperature, they are only weakly dependent on composition, providing that the concentration of solute is not great (<20%) or the diffusivities of the crystallizing component is greater than or equal to that of the solute. This can be seen, for instance, in the growth rate data of Keith and Padden[7].

Figures 15 and *16* show maximum and minimum values of Λ for iPS/aPS and for high/low molecular weight polyethylene blends. These values were computed using measured growth rates[7,35] and diffusivities determined

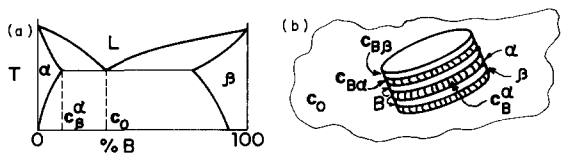

Figure 14 The situation for eutectic solidification in small molecular systems: (a) phase diagram; (b) growing colony of alternating α and β lamellar crystals

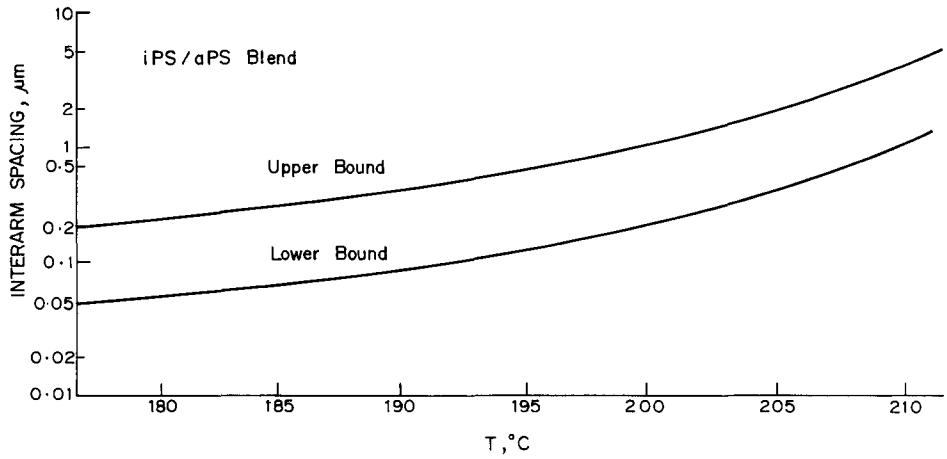

Figure 15 Computed upper and lower bound spherulite inter-arm spacings for a 90:10 iPS/aPS blend crystallizing at 125°C

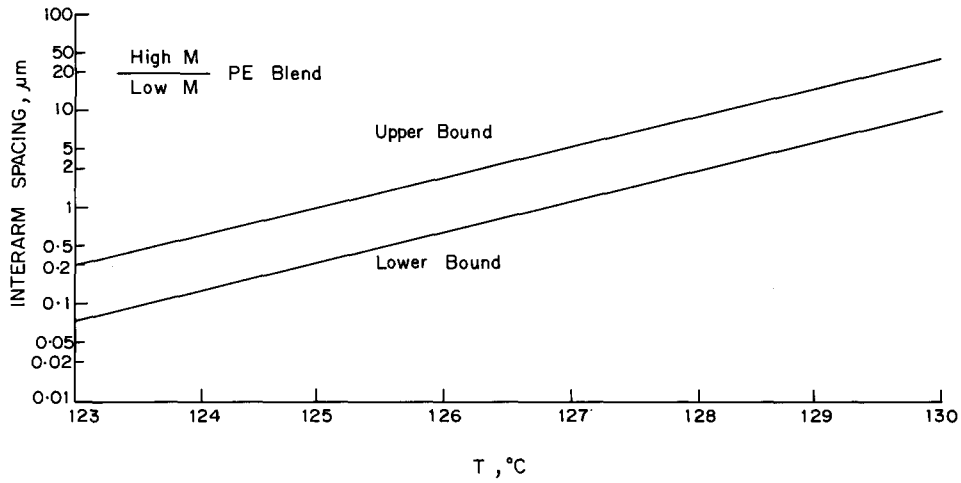

Figure 16 Computed upper and lower bound spherulite inter-arm spacings for an 80:20 high/low molecular weight PE blend crystallizing at 125°C

from the data of Antonietti *et al.*[29] for PS of 60 000 molecular weight and of Bartels *et al.*[34] for polyethylene of 66 000 molecular weight.

The kinetics of densely branched spherulitic structures (*Figure 1c*) require more sophisticated treatment. Such morphologies develop because of the geometrical instability of the dendritic tip. Goldenfeld[11] has put forward an outline of the treatment of this problem, but this must still be developed quantitatively.

CRYSTALLIZATION IN HIGHLY STRAINED SYSTEMS

Background

High-speed fibre spinning and the heat-setting process in conventional spun fibres are archetypal cases of crystallization under very high molecular orientation. In these cases, for example for poly(ethylene terephthalate) (PET), the crystal/non-crystal growth front moves at velocities of at least 75 cm s^{-1} and up to some 15 000 cm s^{-1} and crystallization is observed to occur at temperatures as low as 120°C.

There are three very interesting implications here:

1. With 'solute' diffusivities in the range of 10^{-14}–10^{-10} cm^2 s^{-1}, the solute diffusion length at these growth rates becomes of atomic dimensions. This means that it is impossible for the non-crystallizable molecules to diffuse away fast enough to keep up with the growth front. Consequently, any normally non-crystallizable molecules must be incorporated into the growing crystals. The crystals produced in this way must be highly defective and only metastable. It would require a high driving force to permit such massive defect incorporation.
2. The natural growth rate is orders of magnitude too low to produce the necessary growth-front propagation rates. However, if a diffusionless transformation is possible, crystallization can still occur. For such a diffusionless process to occur, at least the following must be obtained:

(i) The chain repeat units must be already near their ultimate crystalline sites, so that no long-range transport is necessary. This implies that the system be highly oriented; diffusionless processes should occur only in highly elongated systems.
(ii) Normally unincorporable components must be included in the transformed product, unless their mobility is enormously greater than that of the normally crystallizing polymer. Because of the incorporation of such defects, the product will be metastable, and should be capable of further transformation later.
(iii) The effective undercooling must be very great, at least locally, in order to produce a net free energy decrease upon crystallization to the metastable product.
(iv) A molecular mechanism of diffusionless transformation must be available.

A few comments on the occurrence of such diffusionless crystallization and on the requirements (i)–(iv) follow.

Such processes appear to occur in melt-spun fibres. For instance, whereas quiescent crystallization of PET at 120°C occurs with a half-time of 300–1000 s[52], crystallization of oriented PET fibres[27] at the same temperature has a half-time of the order of 0.1 s. Very small half-times of crystallization have likewise been reported for nylon 66 fibres[53]. Van Antwerpen and van Krevelen report spherulite growth velocities in unoriented PET at 140°C of the order of microns per second[52], whereas Hristov and Schultz[54] report crystallization velocities of the order of 100 cm s^{-1} for PET fibres crystallized under axial stress at this temperature. Under such conditions, the crystallization product is very fine (< 10 nm) fibrils whose axes contain the chain and fibre axes[1,27].

Similar results are reported for very thin polymer films drawn directly from the melt under conditions of high lateral constraint and rapid cooling. For instance, fine (~10 nm) fibrillar crystals are invariably formed[14–19]. Again, these crystals formed during the very rapid (tens of milliseconds) cooling of the films to near room temperature.

It is suggested that in these cases, the chains need only 'jostle' slightly to come into near-crystalline registry. A more precisely defined mechanism has not been proposed. Since the motion of the crystallizing molecules is so restricted, kinks and jogs in the chain must be incorporated. In fact, the crystals initially formed exhibit poor crystalline order, indicating the incorporation of defects and/or of defective species. With heat treatment, the defects rapidly migrate, causing formation of a periodic crystal–amorphous sequencing.

The incorporation of normally non-crystallizable molecules into such rapidly growing crystals is normally

necessary, because the diffusion length has shrunk to the dimensions of a few molecular diameters. Let us take such a diffusion length as 1.0 nm. The velocity V^* associated with this diffusion length and a diffusivity of 10^{-12} cm^2 s^{-1} is of the order of 10^{-5} cm s^{-1}, many orders of magnitude below the measured growth rates.

The large driving force may be an entirely thermal one (large undercooling) or it may be assisted by molecular orientation. In the Appendix it is shown that for usual macroscopic draw ratios ($\leqslant 4$), the additional undercooling due to orientation is normally tens of degrees, but this may be locally larger, for instance, near entanglements or at the tip of a growing fibril.

3. The transformation kinetics must become governed by the rate at which the heat of fusion can be removed. Suppose that crystallization is taking place at a velocity of 75 cm s^{-1}, as directly observed in post-spinning treatment of PET fibres[54]. With a thermal diffusivity of 6×10^{-4} cm^2 s^{-1}, the thermal diffusion length will be $< 10^{-5}$ cm. For PET fibres spun at 10000 cm s^{-1} (in the ultra-high-speed spinning range), the thermal diffusion length will be < 1 nm, assuming, as is reasonable, that there is only one crystallization front. Since crystal growth-front dimensions are generally of the order of magnitude of the diffusion length, very fine crystals are expected.

Finally, for molecular orientation to be effective, crystallization must occur before relaxation to a less oriented state can occur. For PET, such relaxation is found to occur in a time of the order of 100 ms. Consequently, processes in which such diffusionless transformations occur must be such that the molecules are in a sufficiently extended state during the crystallization process. Normally this requires a positive stress or strain on the system during the transformation.

Heat flow effects during crystallization in highly oriented systems

From the thermal diffusion length values mentioned above, it becomes clear that a simple spherical or a planar front is not possible; rather, the growth front must break down into fine, fibrous crystals, in order to dissipate the heat of fusion most efficiently. Such behaviour is well known in small molecule systems. The resulting elongated crystals are known as thermal dendrites.

Theories of dendrite growth attempt to predict the relationship between growth velocity V and dendrite tip radius ρ and to generate absolute values for these quantities. Most analyses[20,55,56] begin with the unconstrained growth of a rod of constant tip geometry growing into an infinite melt held at $T_0 < T_m$. This is a steady-state (constant velocity) problem and has been solved analytically for paraboloids of circular[57] and elliptical[58] cross-section. For a crystal with an isothermal tip of circular cross-section. Ivantsov[57] derived the following relationship between V and ρ:

$$-(V\rho/2D_T)\exp(V\rho/2D_T)E_i(-V\rho/2D_T) = (c_p/L)[T(\text{int}) - T_0] \quad (29)$$

where $T(\text{int})$ is the temperature of the non-crystalline phase at the growth surface and $E_i(y)$ is the exponential integral function:

$$E_i(y) = \int_x^\infty (e^{-a}/a)\,da \quad (30)$$

In order to solve for the product $V\rho$, a value of $T(\text{int})$ must be obtained. For a pure substance:

$$T(\text{int}) = T_m[1 - (2\gamma_s/L)/\rho] - \delta T \quad (31)$$

where the term containing ρ and γ_s accounts for capillarity at the tip and δT is the undercooling necessary to drive the interface forward at velocity V. Inserting (31) into (29):

$$-ye^y E_i(-y) = (c_p T_m/L)/[1 - T_0/T_m - (2\gamma_s/L)/\rho - \delta T/T_m] \quad (32)$$

where $y = V\rho/2D_T$. Bolling and Tiller[59] point out that a dendrite growing at constant shape cannot be isothermal. The analysis has been modified[59,60] to account for non-isothermal effects.

For long-chain polymers, another undercooling term, δT_ε, must be incorporated. This term accounts for the effect of chain extension on the undercooling. As shown in the Appendix:

$$\delta T_\varepsilon \cong 3RT(x^2 - 1)/n \quad (33)$$

where x is the relative chain extension (the local draw ratio) and n is the number of flexible segments in the chain. Incorporating (33) into (32), one has:

$$-ye^y E_i(-y) = (c_p T_m/L)[1 - (T_0 + \delta T + \delta T_\varepsilon)/T_m - (2\gamma_s/L)] \quad (34)$$

Algebraically, the effect of chain extension is as a simple decrement to the far-field temperature T_0.

While (34) can be solved to obtain a relationship between V and ρ, another principle must be invoked to establish absolute values. Such principles are generally attempted answers to the question 'How does nature decide what velocity (or radius) to choose?' Some attempted solutions include maximum entropy production[59], maximum growth velocity[59–61] and, most recently, marginal stability[20,62,63].

In the case of fibre spinning, the fibre is effectively moved through a temperature gradient. This situation is depicted in *Figure 17*. In this case, a growth front is stable in laboratory space, at some temperature at which the diffusion-controlled growth velocity matches the spinline velocity. Here V has an exothermally imposed value and (34) can be solved to find the relationship between V and the crystallization temperature.

Two modifications to equation (34) are to be made in this case: the δT term can be ignored, since there is no thermal impediment to the conjectured diffusionless growth, i.e. V_n is without bound; the heat of fusion L is

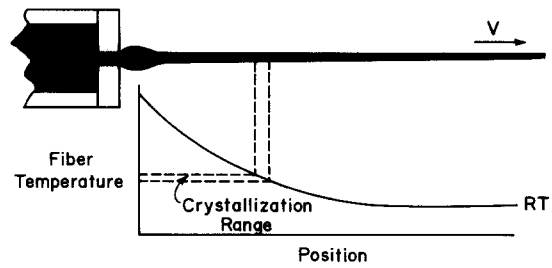

Figure 17 Schematic of a melt-spinning fibre threadline and of the temperature along the fibre

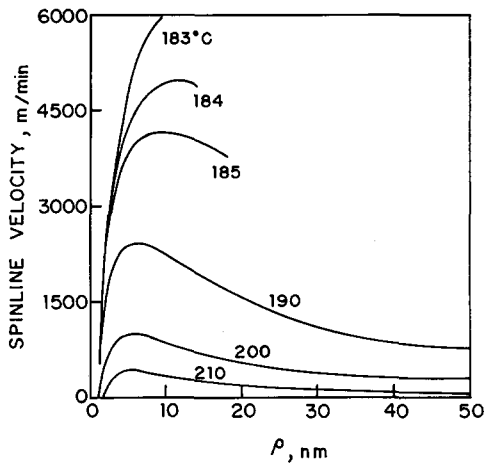

Figure 18 Computed PET spinline crystallization velocity *versus* dendrite tip radius at several temperatures

effectively lowered through the incorporation of defects in the product crystal. This effect has been incorporated in the treatment of Tiller and Schultz[13].

In practice, one uses (34) to obtain the $V-\rho$ relationship for possible crystallization temperatures T. These results are then used to determine absolute values of T and ρ. To a first approximation, (34) is used without the V/β term and without including a defect term. Such a set of solutions is shown in *Figure 18*, using parameters appropriate to PET fibres solidifying isothermally. The parameters used are given in *Table 1*.

It is useful to look in some detail at *Figure 18*. At each temperature, there are two values of crystallite tip radius associated with each velocity. This bifurcation reflects two possible ways in which L can be dissipated at a rate consistent with the imposed transformation front velocity. One way is to form filamentary crystals narrow enough to dissipate the heat three-dimensionally. In this case, the heat is dissipated so efficiently that the temperature gradient beyond the tip is relatively small. The other way is to operate at a sufficiently large tip radius that the thermal gradient remains large and the consequent heat flux also relatively large. At any temperature, the tip radii associated with these two mechanisms approach each other as the velocity increases. Finally, there is a critical velocity at which the two branches merge and above which heat cannot be dissipated rapidly enough to maintain the imposed crystallization rate.

The critical velocity increases with decreasing temperature. Below 185°C the critical velocity increases very steeply with temperature.

The tip radius associated with the critical velocity increases with the critical velocity.

Consider now what happens in a spinline. As a volume element moves away from the spinneret, it experiences a continuously decreasing temperature and a continuously increasing elongational stress. George has shown that the temperature gradient along the fibre is nearly independent of take-up speed (at constant spinneret throughput)[64]. At low spinline velocities, the fibre diameter decrease is gradual and is predictable on a macroscopic model of the material and heat flows. However, above a critical take-up speed, the region of diameter decrease becomes localized in a narrow neck[64–66]. According to the present model, in this narrow zone the local molecular orientation is sufficiently high to trigger diffusionless transformation. The actual crystallization in this zone occurs at a velocity given by the local spinline velocity and at a temperature and crystalline fibril diameter dictated by local heat flow.

As the volume element moves downstream from the spinneret, it encounters lower and lower temperatures. Associated with these temperatures is a critical velocity, above which crystallization cannot take place (*Figure 18*), since the heat of fusion cannot be removed rapidly enough. When the local temperature is such that the critical velocity matches the local spinline velocity, then crystallization can take place. In this way, the crystallization temperature and the crystallite diameter are fixed by the critical velocity.

Figure 19 shows the crystallization temperature and crystal tip radius, determined from *Figure 18*. Over the region of spinline crystallization ($>3500\ m\ min^{-1}$) the crystallization temperature is effectively constant, at 183°C, while the filament radius increases with spinline velocity. It is to be emphasized at this point that the computations leading to *Figures 18* and *19* are based on values of thermal diffusivity and surface energy which may or may not match the actual values of the highly oriented systems under analysis. Nevertheless, the predicted crystallite size and the crystallization temperature are of the correct magnitudes. Furthermore, in the computations of *Figure 18*, the effective undercooling was not allowed to vary with spinline velocity. The effect of this simplification is treated below. More detailed correlation with experiment is now examined.

Figure 20 shows experimental crystallite diameters, obtained by several authors[67–69] from X-ray diffraction data, using the Scherrer formula. The broken line curves are the values predicted by equation (34), using different values of surface energy and thermal diffusivity (similar to, but different from, those of *Table 1*). Both experimental and predicted values increase with spinline velocity, but the theoretical curves show a low velocity asymptote not found in the experimental results.

Figure 21 shows experimental crystallization temperatures (actually heat-flow computations based on measured spinline diameter measurements) *versus* spinline velocity. While the data of Heuvel and Huisman[67] lie above the prediction, those of Shimizu *et al.*[70] and of George[64] lie below. This is not too surprising, since the temperature at which crystallization takes place is known to be strongly affected by molecular weight and chain branching[68,71]. Further, the entropy of fusion, L/T_m, is an important parameter in the computed temperature of crystallization, but may be itself a function of orientation and defect incorporation.

While the absolute value comparison between predicted and 'measured' temperature is acceptable, it

Table 1 Material parameters used in PET fibre velocity computation. (Thermodynamic parameters taken from D. W. van Krevelen, 'Properties of Polymers', Elsevier, Amsterdam, 1976)

c_p (cal $mol^{-1}\ °C^{-1}$)	94.1
L (cal mol^{-1})	5820
ρ_m (g cm^{-3})	1.33
T_m (°C)	518
n	200
x	6.4
D_T ($cm^2\ s^{-1}$)	0.58×10^{-3}

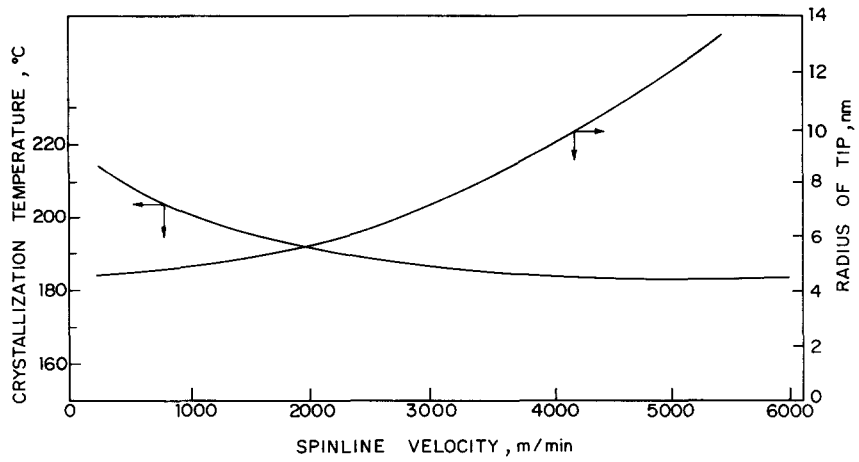

Figure 19 Crystallization temperature and crystal tip radius computed for the melt-spinning of PET fibres

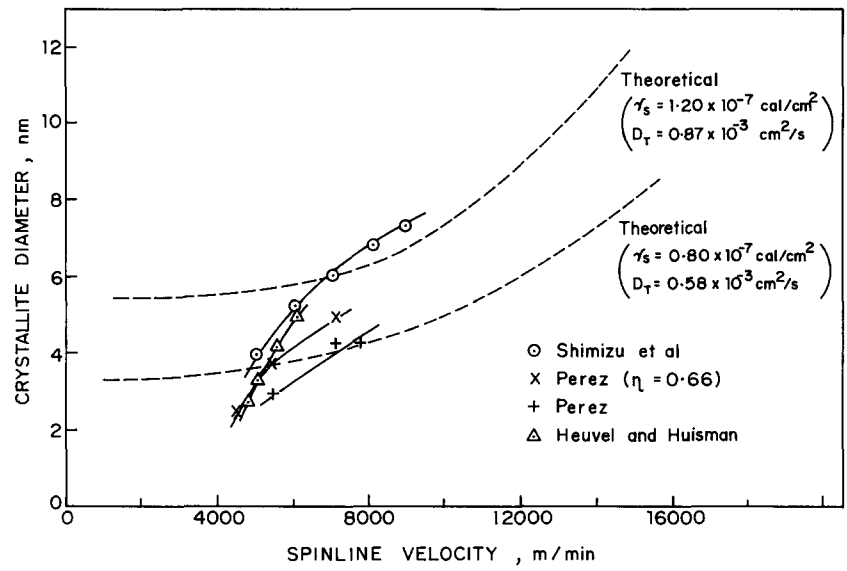

Figure 20 Computed and measured PET crystallite diameter *versus* spinline velocity. The measured velocities are taken from Heuvel and Huisman[67], Perez[68] and Shimizu *et al.*[69]

is clear that the trends of solidification temperature *versus* threadline velocity are different between experiment and prediction. This is, however, expected. In the computations, the actual melt temperature T_0 was not used; what was used was the difference $T_0-\delta T$. In order to obtain the actual melt temperature, it is necessary to add the 'orientation undercooling' δT to the values in *Figure 21*. It is to be expected that δT will increase with spinline velocity. Hence an upward trend in T_0, to a level some 30°C above the computed 182°C is reasonable. In that case, the computed temperatures align reasonably well with those reported by Heuvel and Huisman[67].

The above comparisons between prediction and experiment justify only the possibility of the quantitative correctness of the analysis. However, no absolute test can be made until truly appropriate values of the thermodynamic variables are made.

CONCLUSIONS

Both rejected chemical species ('solute') and the heat of fusion must be dissipated as a crystal growth front moves forward. The natural velocity of the front is defined by the thermodynamic driving force. Attainment of the natural velocity can be made difficult by sluggishness in the dissipative processes. Interface geometries with sharp asperities may form to assist the diffusional processes. Thus, the flow of 'solute' or heat can act to shape the growth front and the final microstructure. A good gauge as to whether a dissipative process will act to control the microstructure is the diffusion length D/V_d. When the diffusion length is significantly greater than the size of the growing entity, there should be no effect of the dissipative process on the microstructure. But when the diffusion length becomes of the same order as or smaller than the growing entity, new crystallization patterns must be formed.

A simple application of this principle allows one to predict whether spherulites of a given material, growing under specific conditions should be microscopically smooth or should be composed of growth arms. Further, a transition from smooth to armed spherulites is predicted for the crystallization of some materials.

The arms of a spherulite are properly modelled as cooperating dendrites, but a simpler model is that of a eutectic system. Using the latter analogy, the character-

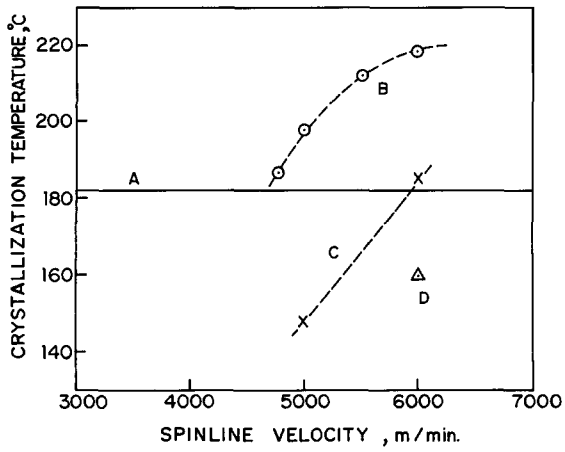

Figure 21 Computed (A) and measured PET crystallization temperatures *versus* spinline velocity. The measured crystallization temperatures are taken from (B) Heuvel and Huisman[67], (C) George[64] and (D) Shimizu *et al.*[70]

istic dimension Λ of the growth arm can be predicted simply. Again, the diffusion length is the important parameter. In general, Λ should increase with increasing crystallization temperature.

When crystallization occurs under conditions of very high molecular strain, crystallization velocities are very large and three conclusions are drawn. First, under such conditions, it is not possible for normally non-incorporable matter to diffuse away from the interface; it must be incorporated. Second, a diffusionless transformation must exist for such rapid transformation to occur. Third, heat flow must control the microstructure, which is dendritic in character. Application of the analysis for thermal dendrite growth permits a relationship among temperature, growth velocity and dendrite tip radius to be written. This analysis has been applied to crystallization in a high-speed spinline. In order to predict absolute values of the dendrite tip radius and the crystallization temperature, a principle of minimum undercooling has been used. Values computed from this analysis are in line with measurement.

ACKNOWLEDGEMENTS

The author is grateful to the National Chemical Laboratory of India (NCL) and its parent organization, the Council on Scientific and Industrial Research, for the opportunity to develop the ideas embodied in this work. Special thanks go to Dr R. A. Mashelkar, Director of NCL, who encouraged this research visit.

REFERENCES

1 Murray, R., Davis, H. A. and Tucker, P. *J. Appl. Polym. Sci.* 1978, **33**, 177
2 Chang, H. *PhD Dissertation* University of Delaware, 1991
3 Martuscelli, E., Canetti, M., Vicini, L. and Seves, A. *Polymer* 1982, **23**, 331
4 Silvestre, C., Cimmino, S., Martuscelli, E., Karasz, F. E. and MacKnight, W. J. *Polymer* 1987, **28**, 1190
5 Keith, H. D. and Padden Jr, F. J. *J. Appl. Phys.* 1963, **34**, 2409
6 Keith, H. D. and Padden Jr, F. J. *J. Appl. Phys.* 1964, **35**, 1270
7 Keith, H. D. and Padden Jr, F. J. *J. Appl. Phys.* 1964, **35**, 1286
8 Keith, H. D. and Padden Jr, F. J. *J. Polym. Sci., Polym. Phys. Edn* 1987, **25**, 229
9 Keith, H. D. and Padden Jr, F. J. *J. Polym. Sci., Polym. Phys. Edn* 1987, **25**, 2265
10 Calvert, P. D. *J. Polym. Sci., Polym. Lett. Edn* 1983, **21**, 467
11 Goldenfeld, N. *J. Cryst. Growth* 1987, **84**, 601
12 Tanaka, H. and Nishi, T. *Phys. Rev. Lett.* 1985, **55**, 1102
13 Tiller, W. A. and Schultz, J. M. *J. Polym. Sci., Polym. Phys. Edn* 1984, **22**, 143
14 Petermann, J. and Gohil, R. M. *J. Mater. Sci.* 1979, **14**, 2260
15 Petermann, J. and Gohil, R. M. *J. Polym. Sci., Polym. Lett. Edn* 1980, **18**, 781
16 Petermann, J. *Makromol. Chem.* 1981, **182**, 613
17 Petermann, J., Gohil, R. M., Schultz, J. M., Hendricks, R. W. and Lin, J. S. *J. Mater. Sci.* 1981, **16**, 265
18 Rau, J., Gohil, R. M., Petermann, J. and Schultz, J. M. *Colloid Polym. Sci.* 1981, **259**, 241
19 Petermann, J., Gohil, R. M., Schultz, J. M., Hendricks, R. W. and Lin, J. S. *J. Mater. Sci.* 1981, **16**, 265
20 Langer, J. S. *Rev. Mod. Phys.* 1980, **52**, 1
21 Hoffman, J. D., Frolen, L. J., Ross, G. S. and Lauritzen, J. I. *J. Res. Natl. Bur. Std.* 1975, **79A**, 671
22 Lauritzen, J. I. and Hoffman, J. D. *J. Res. Natl. Bur. Std.* 1960, **64A**, 73
23 Hoffman, J. D. and Lauritzen, J. I. *J. Res. Natl. Bur. Std.* 1961, **65A**, 297
24 Turnbull, D. and Fisher, J. C. *J. Chem. Phys.* 1949, **17**, 71
25 Carslaw, H. S. and Jaeger, J. C. 'Conduction of Heat in Solids', Oxford University Press, London, 1959, Ch. XI
26 National Bureau of Standards, 'National Bureau of Standards Applied Mathematics Series No. 23: Tables of Normal Probability Functions', US Government Printing Office, Washington DC, 1953
27 Peszkin, P. N., Schultz, J. M. and Lin, J. S. *J. Polym. Sci., Polym. Phys. Edn* 1986, **24**, 2591
28 Boon, J., Challa, G. and van Krevelen, D. W. *J. Polym. Sci.* 1968, **6A** (2), 1791
29 Antonietti, M., Coutandin, J., Grütter, R. and Sillescu, H. S. *Macromolecules* 1984, **17**, 798
30 Mills, P. J., Green, P. F., Palmstrøm, C. J., Mayer, J. W. and Kramer, E. J. *J. Polym. Sci., Polym. Phys. Edn* 1986, **24**, 1
31 Anderson, J. E. and Jou, J.-H. *Macromolecules* 1987, **20**, 1544
32 Klein, J. and Briscoe, B. J. *Proc. R. Soc. (London)* 1979, **A365**, 53
33 Klein, J. *Phil. Mag.* 1981, **43**, 771
34 Bartels, C. R., Crist, B. and Graessley, W. W. *Macromolecules* 1984, **17**, 2702
35 Rego Lopez, J. M., Conde Brana, M. T., Terselius, B. and Gedde, U. W. *Polymer* 1988, **29**, 1045
36 Mullins, W. W. and Sekerka, R. F. *J. Appl. Phys.* 1963, **34**, 323
37 Mullins, W. W. and Sekerka, R. F. *J. Appl. Phys.* 1964, **35**, 444
38 Sekerka, R. F. *J. Phys. Chem. Solids* 1957, **28**, 983
39 Sekerka, R. F. in 'Crystal Growth' (Ed. H. S. Peiser), Pergamon, Oxford, 1967
40 Coriell, S. R. and Parker, R. L. in 'Crystal Growth' (Ed. H. S. Peiser), Pergamon, Oxford, 1967
41 Sekerka, R. F. in 'Crystal Growth, an Introduction' (Ed. P. Hartman), North-Holland, Amsterdam, 1973
42 Woodruff, D. P. 'The Solid–Liquid Interface', Cambridge University Press, Cambridge, 1973
43 Langer, J. S. and Turski, L. A. *Acta Metall.* 1977, **25**, 1113
44 Langer, J. S. *Acta Metall.* 1977, **25**, 1121
45 Keith, H. D. and Padden Jr, F. J. *Polymer* 1986, **27**, 1463
46 Laxmanan, V. *Acta Metall.* 1985, **33**, 1037
47 Trivedi, R. and Somboonsuk, K. *Acta Metall.* 1985, **33**, 1061
48 Burden, M. H. and Hunt, J. D. *J. Cryst. Growth* 1974, **22**, 109
49 Trivedi, R. *J. Cryst. Growth* 1980, **49**, 219
50 Kurz, W. and Fisher, D. J. *Acta Metall.* 1981, **29**, 11
51 Shewmon, P. G. 'Transformations in Metals', McGraw-Hill, New York, 1969
52 van Antwerpen, F. and van Krevelen, D. W. *J. Polym. Sci., Polym. Phys. Edn* 1972, **11**, 2423
53 Elad, J. and Schultz, J. M. *J. Polym. Sci., Polym. Phys. Edn* 1984, **22**, 781
54 Hristov, H. A. and Schultz, J. M. *Polymer* 1988, **29**, 1211
55 Doherty, R. in 'Crystal Growth' (Ed. B. R. Pamplin), Pergamon Press, Oxford, 1975
56 Laxmanan, V. *Acta Metall.* 1985, **33**, 1023
57 Ivantsov, G. P. 'Growth of Crystals', Consultants Bureau, New York, 1958
58 Horvay, G. and Cahn, J. W. *Acta Metall.* 1961, **9**, 695
59 Bolling, G. F. and Tiller, W. A. *J. Appl. Phys.* 1961, **32**, 2587
60 Nash, G. E. and Glicksman, M. E. *Acta Metall.* 1974, **22**, 1283
61 Glicksman, M. E., Schaefer, R. J. and Ayers, J. D. *Metall. Trans.* 1976, **A7**, 1747

62 Langer, J. S. and Müller-Krumbhaar, H. *J. Cryst. Growth* 1977, **42**, 11
63 Langer, J. S. and Müller-Krumbhaar, H. *Acta Metall.* 1978, **26**, 1681, 1689, 1697
64 George, H. H. *Polym. Eng. Sci.* 1982, **22**, 292
65 Perez, G. and Lecluse, C. in 'Proceedings of the International Man-Made Fiber Conference', Dornbirn, Austria, 20–22 June 1979
66 George, H. H., Hole, A. and Buckley, A. *Polym. Eng. Sci.* 1983, **23**, 95
67 Heuvel, H. M. and Huisman, R. in 'High Speed Spinning' (Eds A. Ziabicki and H. Kawai), John Wiley, New York, 1985, p. 295
68 Perez, G. in 'High Speed Spinning' (Eds A. Ziabicki and H. Kawai), John Wiley, New York, 1985, p. 333
69 Shimizu, J., Okui, N. and Kikutani, T. in 'High Speed Spinning' (Eds A. Ziabicki and H. Kawai), John Wiley, New York, 1985, p. 429
70 Shimizu, J., Kikutani, T. and Takaku, A. in 'Proceedings of the International Symp. on Fiber Science and Technology', Hakone, Japan, 20–24 August 1985, Elsevier Applied Science, Barking, 1986, p. 62
71 Perez, G. and Jung, E. in 'Proceedings of the International Symp. on Fiber Science and Technology', Hakone, Japan, 20–24 August 1985, Elsevier Applied Science, Barking, 1986, p. 62
72 Schultz, J. M. 'Polymer Materials Science', Prentice-Hall, Englewood Cliffs, New Jersey, 1974

APPENDIX

Effect of chain stretching on the effective undercooling

In highly strained materials, the entropy of the initial non-crystalline material is decreased and its free energy increased, relative to the quiescent melt. Increasing the free energy of the non-crystalline phase, via deformation, results in an increase in the melting point and, consequently, in the effective undercooling. In what follows, a simple random-walk treatment of a freely jointed chain is used. While this should be only a first approximation to reality, it should serve to demonstrate the principle and to produce effective undercooling values which are also correct to a first approximation.

For a freely jointed chain, the number of complexions of a chain extended in the x-direction to a chain end-to-end length R_x is given by[72]:

$$W(R_x) = (2/\pi n)^{1/2} 2^n \exp[-R_x^2/2(R_x^2)_0] \quad \text{(A1)}$$

where $(R_x^2)_0$ is the mean square x component of the chain end-to-end distance of a chain in an unperturbed system. Thus S_e, the entropy per chain of a chain extended by a stretch $x = R_x/(R_x)_0$ is:

$$S_e = k \ln[W(R_x)] \quad \text{(A2)}$$

where k is Boltzmann's constant. The effect of stretching an uncrystallized chain is to reduce its entropy. Consequently, the entropy of the non-crystallized material more closely approaches that of the crystal, the free energy difference between the two phases increases, and the effective melting point is increased from T_m to T'_m. The molar free energy change upon crystallizing a chain in the perturbed state is then:

$$\Delta G = -L(T'_m - T)/T'_m + (RT/n) \ln[W(R_x)/W(R_x)_0] \quad \text{(A3)}$$

where n is the number of flexible segments in a chain. Combining equations (29)–(31), we have:

$$\Delta G = -L(T'_m - T)/T'_m = -RT(x^2 - 1)/n \quad \text{(A4)}$$

The effective melting point T'_m is determined by setting $\Delta G = 0$. Thus:

$$-L(T'_m - T)/T'_m = -RT(x^2 - 1)/n \quad \text{(A5)}$$

Rearranging (33), the effective undercooling is found to be:

$$T'_m - T = T\{1/[1 - (RT/2Ln)(x^2 - 1)] - 1\} \quad \text{(A6)}$$

Using thermodynamic values for PET (see *Table 1*), various chain lengths, and a temperature of 453 K (55 K below T_m), the effective undercooling has been computed. The results are shown in *Figure A1*. What is seen is that relatively low chain lengths ($n < 400$) and relatively large chain extensions ($x = 3$) are required to produce substantial undercooling. However, these conditions are met in polyester spinlines and orientational undercoolings of tens of degrees should be experienced. Further, if the strain is extremely inhomogeneous, as it may be in the vicinity of entanglement points and at the growth front, the effective undercooling may be even greater. An orientational undercooling of 20–30°C is reasonable in the spinning of PET.

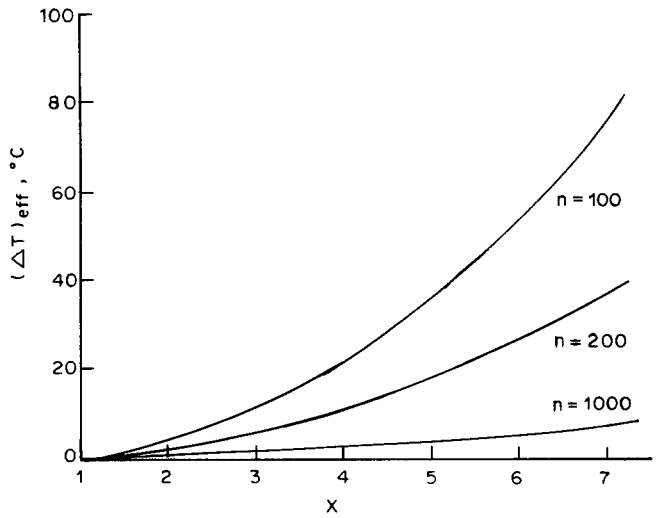

Figure A1 Increase in the effective undercooling with respect to the local draw ratio x, computed according to a simple Gaussian chain model with no relaxation